

Cascading Failures in Interdependent Lattice Networks: The Critical Role of the Length of Dependency Links

Wei Li,¹ Amir Bashan,² Sergey V. Buldyrev,³ H. Eugene Stanley,¹ and Shlomo Havlin^{1,2}

¹Center for Polymer Studies and Department of Physics, Boston University, Boston, Massachusetts 02215, USA

²Department of Physics, Bar-Ilan University, Ramat-Gan 52900, Israel

³Department of Physics, Yeshiva University, 500 West 185th Street, New York, New York 10033, USA

(Received 26 December 2011; published 31 May 2012)

We study the cascading failures in a system composed of two interdependent square lattice networks A and B placed on the same Cartesian plane, where each node in network A depends on a node in network B randomly chosen within a certain distance r from the corresponding node in network A and vice versa. Our results suggest that percolation for small r below $r_{\max} \approx 8$ (lattice units) is a second-order transition, and for larger r is a first-order transition. For $r < r_{\max}$, the critical threshold increases linearly with r from 0.593 at $r = 0$ and reaches a maximum, 0.738 for $r = r_{\max}$, and then gradually decreases to 0.683 for $r = \infty$. Our analytical considerations are in good agreement with simulations. Our study suggests that interdependent infrastructures embedded in Euclidean space become most vulnerable when the distance between interdependent nodes is in the intermediate range, which is much smaller than the size of the system.

DOI: 10.1103/PhysRevLett.108.228702

PACS numbers: 89.75.Hc

Most previous studies of the robustness of interdependent networks [1–19] focused on random networks in which space restrictions are not considered. Most real networks are embedded either in two-dimensional or in three-dimensional space, and the nodes in each network might be interdependent with nodes in other networks. One example is a computer in a computer network, which is dependent for power upon the functioning of a local power grid network where both networks are spatially embedded. Another example is the way the worldwide network of seaports embedded in the two-dimensional surface of the earth is interdependent with power grid networks embedded on the same surface. A seaport needs electricity from a nearby power station to operate, and a power station needs fuel supplied through a nearby seaport to operate. Thus, the failure of a power station in a power grid network will cause a failure in a nearby seaport and vice versa. Space constraints, such as the network dimensionality [20], influence the network properties dramatically, and thus the question about the resilience of interdependent spatial networks is of much interest.

The case of interdependent spatially embedded networks is significantly different from interdependent random networks in two ways: (i) within each network, nodes are connected only to the nodes in their spatial vicinity, while in the randomly connected networks, the concept of spatial vicinity is not defined; (ii) the dependency links establishing the interdependence between the networks might not be random but may have a typical length r . To understand how these space constraints affect the resiliency of interdependent networks, we study the mutual percolation of a system composed of two interdependent, two-dimensional lattices A and B , where a node A_i can connect to its dependent node B_j only within distance r

from A_i (see Fig. 1). Since a node can be functional only if it is connected to the network, the resilience can be measured, using percolation theory, as the size of the remaining giant component after an attack on the network.

Our model consists of two identical square lattices A and B of linear size L and $N = L^2$ nodes with periodic boundary conditions. In each lattice, each node has two types of links: connectivity links and dependency links. Each node is connected to its four nearest neighbors within the same lattice via connectivity links. Also, a node A_i located at (x_i, y_i) in lattice A is connected with one and only one node B_j located at (x_j, y_j) in lattice B via a bidirectional

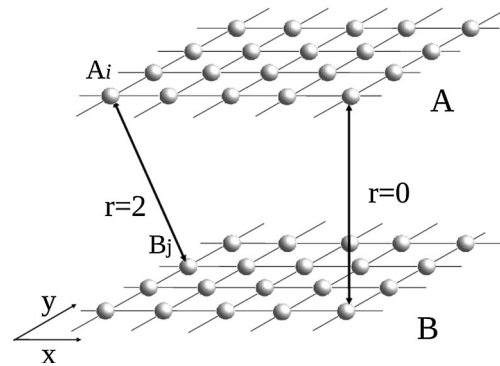


FIG. 1. Two square lattices A and B where in each lattice every node has two types of links: connectivity links and dependency links. Every node is initially connected to its four nearest neighbors within the same lattice via connectivity links. Also, each node A_i in lattice A depends on one and only one node B_j in lattice B via a dependency link (and vice versa), with the only constraint that $|x_i - x_j| \leq r$ and $|y_i - y_j| \leq r$. If node A_i fails, then node B_j fails. If node B_j fails, then node A_i fails. Network A is shifted vertically for clarity.

dependency link, with the only constraint that $|x_i - x_j| \leq r$ and $|y_i - y_j| \leq r$ (Fig. 1). The parameter r represents the maximum distance a node in one network gets support from a node in another network.

Although real networks embedded in two-dimensional space may have more complex structures than the square lattice, our model can serve as a benchmark for more complex situations. Moreover, it is known that the percolation transition in two dimensions has universal scaling behavior which does not depend on the coordination number and is the same for lattice and off-lattice models, as long as the links have a finite characteristic length. Hence, mutual percolation in two dimensions should not depend on the particular realization of the model [21].

The difference between connectivity and dependency links is that for connectivity links, a node fails only when it does not belong to the giant cluster of its network, while for dependency links, a node fails once the node on which it depends in the other network (connected via a dependency link) fails. An initial random attack destroys a fraction $1 - p$ of nodes in network A . This causes a certain number of nodes to disconnect from the giant component of network A so that only a fraction of nodes $p_1 = P_\infty(p)$ remains functional. Here $P_\infty(p)$ is the order parameter of conventional percolation in a square lattice [21]. The removal of nodes in network A causes the removal of the dependent nodes in network B . As a result, only a fraction $P_\infty(p_1)$ of nodes in network B remains functional. This produces additional damage in network A and so on. The cascading failure process stops when no further damage propagates between the lattices. If the length of dependency links is totally random ($r = L$), the formalism developed in Ref. [1] can be applied. This is because at the i th stage of the cascade the resulting giant component $P_\infty(p_i)$ is the order parameter of conventional percolation computed for a random fraction of nodes p_i surviving after all the nodes in one network that depend on the nonfunctional nodes of the other network are removed. Accordingly, we can represent the cascading failure by the recursive equations for the survived fraction p_i ,

$$\begin{aligned} p_0 &= p, \\ p_1 &= \frac{p}{p_0} P_\infty(p_0) = P_\infty(p), \\ &\vdots \\ p_i &= \frac{p}{p_{i-1}} P_\infty(p_{i-1}). \end{aligned} \quad (1)$$

The recursive steps of Eq. (1), representing the cascading failures in the giant component shown in Fig. 2, are in good agreement with simulations. In the limit $i \rightarrow \infty$, Eq. (1) yields the equation for the mutual giant component at steady state, $\mu \equiv P_\infty(p_\infty)$,

$$x = \sqrt{p P_\infty(x)}, \quad (2)$$

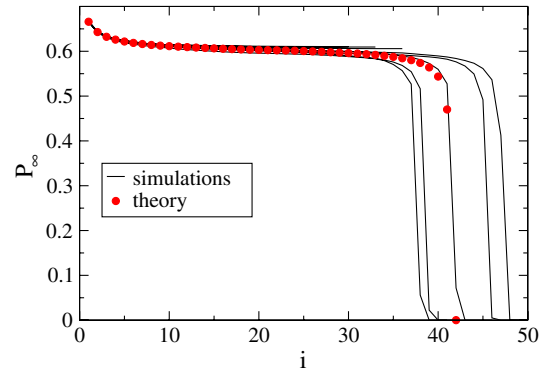


FIG. 2 (color online). Giant component size P_∞ as a function of step i at the first-order transition regime at $p = 0.6825$ for $r = L = 1000$. The simulation results (solid lines) are in good agreement with the theoretical results (dots). The value of p is close to the percolation threshold $p_c^\mu = 0.6827$.

where $x \equiv p_\infty$. Using the form of $P_\infty(x)$ for conventional percolation obtained from numerical simulations, Eq. (2) can be solved graphically as shown in the inset of Fig. 3. Due to the specific shape of the function $P_\infty(p)$ [see Fig. 3], ($P_\infty(p) < p$, $\lim_{p \rightarrow 1} P_\infty/p = 1$, $\lim_{p \rightarrow p_c} P_\infty(p) = 0$, and $p_c = 0.5927$ for square lattice), it does not have solutions for a small p except for the trivial case $x = 0$.

Figure 3 shows the numerical solution of Eq. (2), which is in good agreement with simulations and compares it with $P_\infty(p)$ of a single network. The critical p for which the nontrivial solution ceases to exist, $p \equiv p_c^\mu$, corresponds to the case when the right-hand side of Eq. (2) becomes tangential at the point of their intersection $x = x_c$ to its left-hand side (Fig. 3 inset). Hence,

$$P_\infty'(x_c)x_c = 2P_\infty(x_c), \quad (3)$$

from which the critical p for mutual percolation is

$$p_c^\mu = x_c^2/P_\infty(x_c). \quad (4)$$

Numerical solutions of Eqs. (3) and (4) yield $p_c^\mu = 0.683$, $x_c = 0.641$, and $P_\infty(x_c) = 0.602$, in good agreement with simulations of the mutual percolation on lattices for $r = L$ as seen in Fig. 3. Figure 3 shows a discontinuity in the order parameter of mutual percolation $\mu(p) = P_\infty(p)$ at $p = p_c^\mu$, which drops from $\mu(p) = 0.602$ to zero for $p < p_c^\mu$, characteristic of a first-order transition.

Next, we study the mutual percolation for different dependency lengths r . An infinite coupling distance $r = \infty$ corresponds to the scenario of random dependency links between the lattices discussed above. For $r = 0$, every failed node in network A leads to removal of a node in network B in the same location. Thus, the percolation clusters in the two lattices are identical and there is no feedback failure in network A . Therefore, the case of $r = 0$ is identical to the case of conventional percolation in noncoupled lattices. Figures 4(a) and 4(b) show the

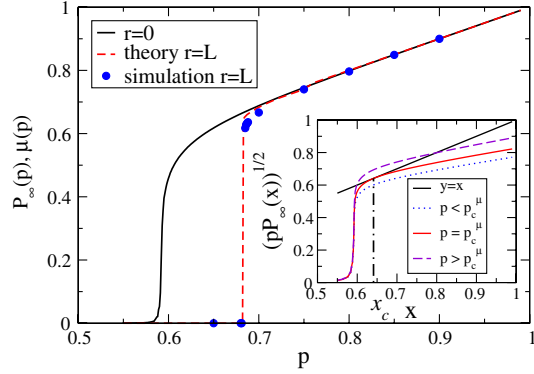


FIG. 3 (color online). The giant component size P_∞ as a function of remaining fraction of nodes p . The solid curve is for conventional percolation on a single square lattice, which also describes the limiting case of $r = 0$. The solid curve is obtained by numerical simulations on $N = 4000 \times 4000$ lattice sites with periodic boundary conditions and averaged over 100 realizations. The dash curve represents the theoretical result $\mu(p)$ for two interdependent lattice networks with $r = L$ given by Eq. (2). The simulation results (dots) are for two interdependent lattice networks with $N = 1000 \times 1000$ and $r = L$. Inset: A schematic graphical solution of Eq. (2) is shown. The curves are $\sqrt{pP_\infty(x)}$ for different p and the solution of Eq. (2) is given by the intersection of the solid curves and the straight line $y = x$. The critical $p = p_c^\mu$ corresponds to the case when the solid curve is tangential to the straight line $y = x$. Numerical solutions of Eqs. (3) and (4) yield $x_c = 0.641$, $P_\infty(x_c) = 0.602$, and $p_c^\mu = 0.6827$.

structure of the giant component just above p_c^μ for very small r (few lattice units) and for $r = L$, respectively. For small r , the structure is similar to the heterogeneous fractal-like giant component of a single network [21]. In contrast, for r of the order of L , the giant component is homogeneous and almost compact [see Fig. 4(b)] but, surprisingly, on the verge of a sudden collapse as a first-order transition. For intermediate values of r , the collapse occurs in a very different way. Figures 4(c)–4(e) show for intermediate values of r (discussed below) that the initial cascade of failures is localized to a region of size r [Fig. 4(c)]. Because of local density fluctuations, the effective fraction of nodes p in one region can be smaller than the overall average, and therefore small clusters at this region become isolated from the giant component and fail even when the entire lattice is still connected. As soon as a region of size r fails, the system becomes unstable: the interface of this bubble starts to expand and soon engulfs the entire system [Figs. 4(d) and 4(e)]. This local effect of a propagating interface owing to finite dependency links increases the system vulnerability compared to the case of random dependency links. Thus we expect $p_c^\mu(r) > p_c^\mu(\infty)$ found for random dependency links. The process of formation of the critical bubble is similar to nucleation near the gas-liquid

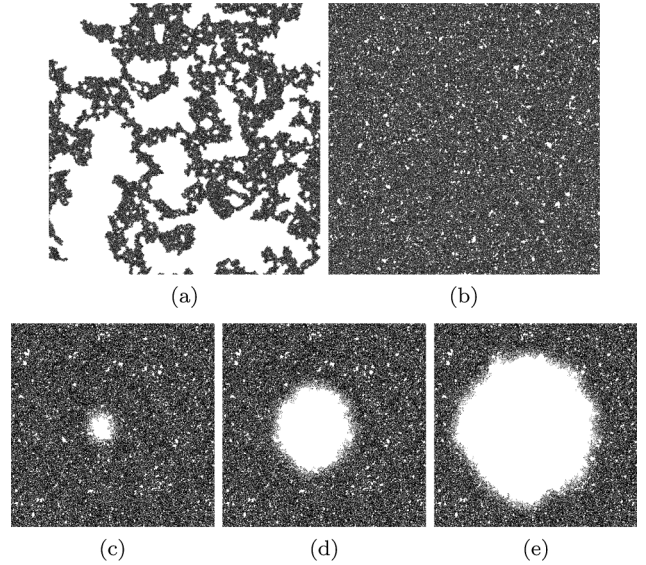


FIG. 4. Three different typical behaviors of interdependent lattices near criticality. Pictures of stable mutual giant component at criticality of two interdependent lattices ($N = 1000 \times 1000$) after cascading failures initiated by a random removal of $1 - p$ of the nodes for (a) $r = 4$ and $p = 0.680$ and for (b) $r = 1000$ and $p = 0.683$. The dynamics of a growing bubble (explained in the text) for $r = 20$ is demonstrated by three snapshots, (c), (d), and (e), of the nonstable giant component of the interdependent lattices ($N = 500 \times 500$) during the cascading process initiated with $p = 0.700$.

spinodal [22]. Thus, it is important to understand the propagation of a flat interface, which would correspond to gas-liquid coexistence.

In order to systematically study the conditions for propagation of a flat interface, we study the two interdependent networks with an empty gap on one edge in lattice A . We construct the two networks with the length of interdependent links less than or equal to r (see Fig. 1). The only difference from our original system is that after random removal of a certain fraction of nodes $1 - p$, we eliminate the nodes in lattice A with coordinates $y_i \leq r$ to create an artificial flat interface. Simulations show that the flat interface freely propagates and that the system totally collapses if $p < p_c^f(r)$, where $p_c^f(r)$ is approximately a linear function of r with $p_c^f(0) = p_c = 0.5927$, $p_c^f(r_f) = 1$, and $r_f \cong 38$. For $r > r_f$, the interface freely propagates through the system even when the lattice is completely intact. This happens because the removed nodes of lattice A above the interface eliminate half of the nodes in lattice B with $y_j \leq r$. Thus, the effective concentration of nodes in lattice B linearly changes from p at distance r from the interface to $p/2$ right at the interface. This system is analogous to percolation in diffusion fronts studied by Sapoval *et al.* [23]. There is thus a certain distance from the interface $r_c = r(2p_c - p)/p$ that corresponds to the critical threshold of conventional percolation. If r_c is much larger than the

typical cluster size in the range between p_c and $p/2$, all the nodes in lattice B in this layer will be disconnected and hence the interface will propagate freely. The interface can stop if $r_c = \xi(p/2)$, i.e., the connectedness correlation length [21] when $p/2$ is less than p_c . We estimate the critical concentration p_c^f from the equation $\xi(p_c^f/2) = r(2p_c - p_c^f)/p_c^f$, which yields $r_f = \xi(1/2)/(2p_c - 1) = 41$ for the case $p = 1$, where $\xi(1/2) = 7.6$ obtained by numerical simulations of conventional percolation on a single lattice. This prediction agrees well with simulations ($r_f \cong 38$). The propagation of the flat interface close to $p_c^f(r)$ is similar to invasion percolation, which is a fractal process with vanishing number of active sites [21], and the average interface velocity approaches zero at $p_c^f(r)$, a characteristic of a second-order transition. Thus, the system completely collapses when (1) a flat interface exists and (2) $p < p_c^f$. The conditions for flat interface propagation, $p_c^f(r)$, were obtained for the artificial model where the flat interface is initially created. However, when the system is initiated by a spatially random removal, a flat interface may be created by random fluctuations over the lattice.

What can we learn from the flat interface behavior on our original system with only initial random failures? When r is large, in the absence of an artificial flat interface, the system does not collapse but rather stays in a metastable state where $p_c^\mu < p < p_c^f$. As soon as $p = p_c^\mu$, a hole of size r is spontaneously formed in a low p regime, and its interface freely propagates through the system because p is already below the critical point p_c^f of the interface propagation. As a result, the interface will completely wipe out the remaining giant component [see Fig. 4(c)–4(e)]. Thus, for large r , the transition is first

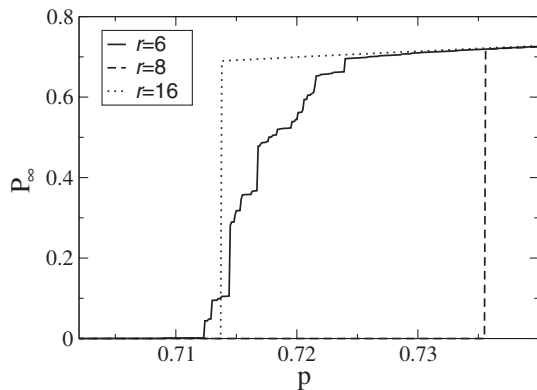


FIG. 5. The fraction of nodes in the giant component as a function of nodes survived after the initial attack. We perform the simulations by gradually removing additional nodes. For $r = 6$, the decrease of giant component occurs in multiple steps, characteristic of a second-order transition. For $r = 8$ and $r = 16$, the giant component may completely collapse by removal of even a single additional node, characteristic of a first-order transition.

order, meaning it is all or nothing, a transition similar to spontaneous nucleation. At these conditions, the removal of even a single additional node may cause the disintegration of the entire system (Fig. 5).

The dynamics of the system becomes completely different for small r . In this case, when p_c^f is small, the characteristic size of the holes ξ_h in the percolation cluster is sufficiently large, and there are many holes of size $\xi_h(p_c^f) > r$. Thus, the flat interface is formed before it begins to propagate. Once p approaches p_c^f from above, the interface begins to propagate simultaneously from all large holes in the system. It can spontaneously stop at any stage of the cascade, leaving any number of sites in the mutual giant component (Fig. 5). The average number of sites in the giant component will approach zero as p approaches p_c^f , subject to strong finite-size effects as in conventional percolation. So for small r , the transition is a second-order, and $p_c^\mu(r) = p_c^f$ linearly increases with r (Fig. 6).

The inset of Fig. 6 shows that at $r = r_{\max}$, $\xi_h(p_c^f(r)) = r \approx 8$, and a flat interface will not spontaneously form. Thus p must be below $p_c^f(r)$ in order for the hole of size r to appear in the system. Once a single hole of such size appears, the flat interface will freely propagate below its critical threshold, wiping out the entire coupled network system, as in a first-order transition. Note that $p_c^\mu(r_{\max}) \approx 0.738 > p_c^\mu = 0.6827$. Thus as r increases, $p_c^\mu(r)$ gradually decreases (Fig. 6). This gradual decrease is caused by two factors. When r increases in the vicinity of r_{\max} , smaller and smaller p is needed in order to create holes of size r . When p becomes close to p_c^μ , the system begins to undergo

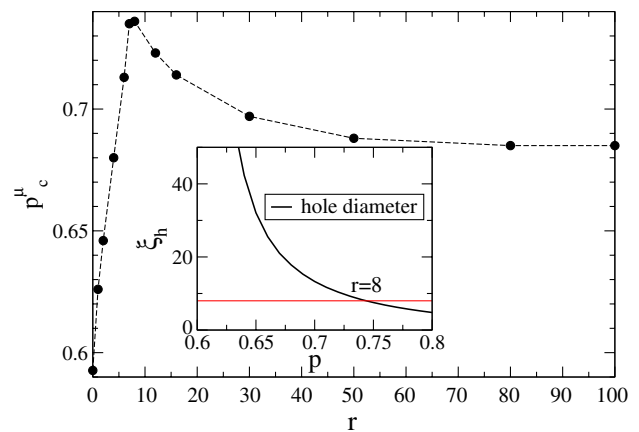


FIG. 6 (color online). The critical p_c^μ as a function of interdependent distance r . The change from second to first order transition occurs at $r_{\max} \approx 8$. The critical p_c^μ of mutual percolation threshold for flat interface and then gradually decreases to $p_c^\mu = 0.683$ at $r = \infty$, which is in good agreement with the theoretical results. Inset: Diameter of the hole size ξ as a function of r on conventional percolation on a single lattice network. $\xi_h \approx r_{\max} = 8$ at $p = 0.744$ is in good agreement with the simulation.

local cascades of failures if the average density in the region of size r falls below p_c^μ . The average over r^2 nodes of this region can deviate from the mean p on the order of a standard deviation $\sqrt{p(1-p)}/r$, thus making the disintegration possible if $p = p_c^\mu(r) \approx p_c^\mu + C/r$, where C is a constant. Note that $p_c^\mu(r)$ has a tendency to increase with the system size. The larger the system, the more likely a sufficiently large hole or a sufficiently large fluctuation in local density will lead to a local cascade of failures.

In summary, our analysis suggests that the change from second-order to first-order transition occurs at $r_{\max} \approx 8$. Note that Ref. [24] found a second-order transition for $r = 0$ on two interdependent lattice networks. Our studies show rich phase transition phenomena when the length of the dependency links r changes. The critical p of mutual percolation increases linearly with r in the range of $r < r_{\max}$ and is characterized by a second-order transition. For $r \geq r_{\max}$, the cascading failures suggest a first-order transition and the critical p gradually decreases to $p_c^\mu = 0.683$ for $r \rightarrow \infty$.

We thank an anonymous referee for comments that improved the paper. We also thank DTRA and ONR for support. S.V.B. acknowledges the partial support of this research through the Dr. Bernard W. Gamson Computational Science Center at Yeshiva College. S.H. thanks the LINC and the Epiwork EU projects, the DFG, and the Israel Science Foundation for support.

-
- [1] S. V. Buldyrev, R. Parshani, G. Paul, H. E. Stanley, and S. Havlin, *Nature (London)* **464**, 1025 (2010).
 - [2] A. Vespignani, *Nature (London)* **464**, 984 (2010).
 - [3] R. Parshani, S. V. Buldyrev, and S. Havlin, *Phys. Rev. Lett.* **105**, 048701 (2010).
 - [4] R. Parshani, C. Rozenblat, D. Ietri, C. Ducruet, and S. Havlin, *Europhys. Lett.* **92**, 68 002 (2010).

- [5] J. Shao, S. V. Buldyrev, S. Havlin, and H. E. Stanley, *Phys. Rev. E* **83**, 036116 (2011).
- [6] E. A. Leicht and R. M. D'Souza, [arXiv:0907.0894](https://arxiv.org/abs/0907.0894).
- [7] C. D. Brummitt, R. M. D'Souza, and E. A. Leicht, *Proc. Natl. Acad. Sci. U.S.A.* **109**, E680 (2012).
- [8] X. Xu, Y. Qu, S. Guan, Y. Jiang, and D. He, *Europhys. Lett.* **93**, 68 002 (2011).
- [9] J. Hao, S. Cai, Q. He, and Z. Liu, *Chaos* **21**, 016104 (2011).
- [10] K. Morino, G. Tanaka, and K. Aihara, *Phys. Rev. E* **83**, 056208 (2011).
- [11] C. Gu, S. Zou, X. Xu, Y. Qu, Y. Jiang, D. He, H. Liu, and T. Zhou, *Phys. Rev. E* **84**, 026101 (2011).
- [12] X. Huang, J. Gao, S. V. Buldyrev, S. Havlin, and H. E. Stanley, *Phys. Rev. E* **83**, 065101(R) (2011).
- [13] J. Gao, S. V. Buldyrev, S. Havlin, and H. E. Stanley, *Phys. Rev. Lett.* **107**, 195701 (2011); *Nature Phys.* **8**, 40 (2012).
- [14] S. V. Buldyrev, N. W. Shere, and G. A. Cwilich, *Phys. Rev. E* **83**, 016112 (2011).
- [15] Y. Hu, B. Ksherim, R. Cohen, and S. Havlin, *Phys. Rev. E* **84**, 066116 (2011).
- [16] R. Parshani, S. V. Buldyrev, and S. Havlin, *Proc. Natl. Acad. Sci. U.S.A.* **108**, 1007 (2011).
- [17] A. Bashan, R. Parshani, and S. Havlin, *Phys. Rev. E* **83**, 051127 (2011).
- [18] A. Bashan and S. Havlin, *J. Stat. Phys.* **145**, 686 (2011).
- [19] J. Gao *et al.*, [arXiv:1108.5515](https://arxiv.org/abs/1108.5515).
- [20] D. Li, K. Kosmidis, A. Bunde, and S. Havlin, *Nature Phys.* **7**, 481 (2011).
- [21] A. Bunde and S. Havlin, *Fractals and Disordered Systems* (Springer, New York, 1991).
- [22] G. Glaser, *Phys. Rev.* **87**, 665 (1952).
- [23] B. Sapoval, M. Rosse, and J. F. Gouyet, *J. Phys. (Paris), Lett.* **46**, 149 (1985).
- [24] S. W. Son, P. Grassberger, and M. Paczuski, *Phys. Rev. Lett.* **107**, 195702 (2011).